AAS 21-595

INTERPLANETARY LOW-THRUST TRAJECTORY DESIGN TO LIBRATION POINT ORBITS VIA SIMS-FLANAGAN TRANSCRIPTION

Yuri Shimane* **and Koki Ho†**

While low-thrust electric propulsion (EP) enables interplanetary missions to deliver larger payload fractions, the orbit insertion phase often necessitates a large, instantaneous ΔV maneuver, rendering it difficult to be conducted by an EP system alone. In contrast, missions to libration point orbits (LPO) may leverage ballistic capture strategies, resulting in no instantaneous ΔV maneuvers required. This work presents a modification to the Sims-Flanagan Transcription for interplanetary low-thrust trajectory design arriving at LPOs by incorporating flexible arrival into an insertion point on their stable manifolds.

INTRODUCTION

Electric propulsion (EP) technology-based low-thrust systems has brought a new dimension of possibility for humanity's activity in space. In the context of space exploration, the exceptionally high specific impulse (I_{sp}) allows for larger payload mass to be delivered. This may translate to more scientific equipment to be brought on-board, or more cargo in the context of space logistics and human spaceflight. Some notable interplanetary exploration missions that benefited from this technology include Dawn, Hayabusa 1 & 2, and Psyche, which are asteroid exploration missions, and BepiColombo, currently heading to Mercury. EP being favored towards applications in exploration of smaller bodies in the solar system may be related to the EP's incapability of providing significant impulsive Δv. Conventionally, a spacecraft approaches its destination with excess energy; then in order to then be captured by the body, an insertion maneuver of significant impulsive Δv is required. An alternative approach is through a weak stability ballistic capture (WSBT), which involves entering the body's sphere of influence at negative specific energy with respect to the body. BepiColombo will employ this strategy upon arrival at Mercury.[1,2] Similarly, insertion into libration point orbits (LPO), which are periodic orbits about libration points of three-body systems, may also be done with much smaller insertion costs, as their manifold structures may be leveraged. This is a particularly remarkable property for spacecraft with EP, as large impulsive Δv requirement can be alleviated.

With EP technology expected to mature further in the upcoming decade, interplanetary missions to large bodies relying entirely on low-thrust propulsion alone will become increasingly sought after as well. Unless the spacecraft must only perform a fly-by in a fashion similar to missions such as Pioneer 10 & 11, Voyager 1 & 2 or New Horizons, a ballistic capture strategy much like

*PhD Student, School of Aerospace Engineering, Georgia Institute of Technology, Atlanta, GA 30332.
†Assistant Professor, School of Aerospace Engineering, Georgia Institute of Technology, Atlanta, GA 30332.

BepiColombo's would be necessary for a low-thrust-only spacecraft to remain at the vicinity of the body.

Several proposals have also been made for exploration missions utilizing Sun-planet system LPOs. The use of the Sun-Mars L1 and L2 halos for establishing a permanent communication link between Earth and space systems in the Martian system has been proposed.[3,4] Tanaka et al considered the Sun-Mars L1 halos as generating mechanisms for WSBC into the Martian system.[5] Shirobokov et al proposed the use of a Sun-Venus L2 halo for placing a space-telescope, permitting earlier detection of potentially hazardous near-earth asteroids (NEAs).[6] Anticipating such applications, this work proposes an approach to design low-thrust interplanetary trajectories that culminate in a ballistic capture upon arrival at its destination. Specifically, the Sims-Flanagan transcription (SFT)[7,8] is modified to incorporate captures into a manifold that brings the spacecraft into the LPO.

SFT is a widely used method for designing interplanetary trajectories that may include gravity assists. Low-thrust propulsion is typically approximated as a series of impulsive maneuvers, thus discretizing the trajectory design problem. While it has been found to be a successful approach in finding complex tours through the solar system, the launch, gravity-assists, and arrival at planetary bodies are parameterized by a $v_\infty \geq 0$ vector relative to the body, which corresponds to parabolic or hyperbolic motion in the vicinity of these bodies.

There has also been development in designing Earth-Mars transfers that incorporate WSBC for high-thrust spacecraft, leveraging Lambert's problem.[9,10] For BepiColombo's approach to Mercury, Jehn et al[1] used ballistic back-propagation from the desired orbit around Mercury matching mission requirements until the spacecraft is outside the sphere of influence of Mercury, which is then matched to the incoming heliocentric transfer.

In the context of more generic WSBC, Toputto et al[11] studied the planar problem to construct interplanetary transfers with impulsive maneuvers for insertion into manifolds. A grid-based interpolation of manifold Poincaré sections has also been proposed for obtaining families of WSBC.[12] The n-stable set of trajectories around a body has been used as a generating mechanism for low-thrust WSBC.[13]

This work extends the SFT to directly construct low-thrust interplanetary transfers that culminate in a ballistic capture. An approach replacing the arrival parameters from the v_∞ vector to a set of variables that model the insertion into a manifold structure is proposed. This insertion point may be located at a pre-defined Poincaré section (PS) along the manifold, or the location of the PS may also be given as a tuning parameter for the optimizer. The propagation of the spacecraft trajectory is replaced by an ODE system with a third-body perturbation to ensure continuity at the insertion point between the heliocentric portion and Sun-planet system portion of the trajectory. The proposed method results in better preliminary estimate of propellant mass required for such an end-to-end low-thrust missions, as both the interplanetary and ballistic capture segments may be considered at the preliminary design level.

This paper is organized as follows. Initially, the two dynamical models used in this work, namely the two-body problem with a third-body perturbation and the restricted three body problem, are introduced. Notions of coordinate transformations, LPOs and invariant manifolds are also discussed. This is followed by an introduction of the SFT, and a detailed description on the modifications made to the traditional formulation to incorporate targeting LPOs. The proposed method is implemented to a mission-design case to a Sun-Venus L2 halo orbit, and optimized solutions are discussed.

BACKGROUND ON THE DYNAMICAL SYSTEM

In order to study interplanetary transfers with ballistic arrivals to LPOs, a heliocentric frame and a Sun-planet circular restricted-three body problem (CR3BP) are considered simultaneously.

Coordinate Frames and Transformations

The heliocentric phase of the transfer is designed in the ecliptic reference frame centered at the Sun, specifically the ECLIPJ2000 frame following JPL's SPICE conventions. In contrast, the approach phase of the transfer is modeled in the CR3BP frame, which is a rotating frame with the x-axis fixed to the Sun-planet line, and the z-axis parallel to the axis of rotation of the planet's orbit. In this frame, the planet's motion around the Sun to be circular.

Given the planet's Keplerian orbital elements argument of perihelion (AOP), true anomaly (TA), inclination (INC), and right-ascension of ascneding node ($RAAN$), transforming a state-vector defined in the CR3BP frame to the ECLIPJ2000 consists of a series of transformations. The first transformation $\boldsymbol{T}_1$ takes the CR3BP state and converts it into an inertial, intermediate state, and its matrix is given by

$$\boldsymbol{T}_1(t) = \begin{bmatrix} \cos \upsilon_1(t) & -\sin \upsilon_1(t) & 0 & 0 & 0 & 0 \\ \sin \upsilon_1(t) & \cos \upsilon_1(t) & 0 & 0 & 0 & 0 \\ 0 & 0 & 1 & 0 & 0 & 0 \\ -\omega_{\text{CR3BP}} \sin \upsilon_1(t) & -\omega_{\text{CR3BP}} \cos \upsilon_1(t) & 0 & \cos \upsilon_1(t) & -\sin \upsilon_1(t) & 0 \\ \omega_{\text{CR3BP}} \cos \upsilon_1(t) & -\omega_{\text{CR3BP}} \sin \upsilon_1(t) & 0 & \sin \upsilon_1(t) & -\cos \upsilon_1(t) & 0 \\ 0 & 0 & 0 & 0 & 0 & 1 \end{bmatrix} \tag{1}$$

where ω_{CR3BP} is the rotational rate of the Sun-planet system, and the rotation angle $\upsilon_1(t)$ is given by $\upsilon_1(t) = AOP + TA(t)$, where the TA has a time-dependency. Then, a rotation $\boldsymbol{T}_2$ about the x-axis by $-INC$ and a final rotation $\boldsymbol{T}_3$ about the z-axis by $-RAAN$ of the position and velocity vectors independently are applied. The combined transformation from CR3BP to ECLIPJ2000, $\boldsymbol{T}_{\text{EC}}(t)$, is given by

$$\boldsymbol{T}_{\text{EC}}(t) = \boldsymbol{T}_3 \boldsymbol{T}_2 \boldsymbol{T}_1(t) \tag{2}$$

While it has not been considered in this work, it is possible to replace the CR3BP with the elliptical restricted three body problem (ER3BP) to account for non-negligible eccentricities of the planet. In this case, the dynamics becomes time-dependent to the position of the planet along its orbit around the Sun, thus care is required when converting a state-vector between the ECLIPJ2000 frame and the ER3BP frame.

Equations of Motion

There are two sets of equations of motion considered in this work. Firstly, the heliocentric two-body equations of motion with a thrust-term are given by

$$\ddot{\boldsymbol{r}} = -\frac{GM}{r^3}\boldsymbol{r} + \frac{\boldsymbol{F}}{m} \tag{3}$$

where GM is the gravitational parameter of the Sun, $\boldsymbol{r}$ is the spacecraft position vector, $\boldsymbol{F}$ is the thrust-vector, and m is the spacecraft mass. If a third-body perturbation due to the presence of a planet is also to be considered, the equations of motion are modified to

$$\ddot{\boldsymbol{r}} = -\frac{GM}{r^3}\boldsymbol{r} + GM_p \left(\frac{\boldsymbol{r}_{sp}}{r_{sp}^3} - \frac{\boldsymbol{r}_p}{r_p^3} \right) + \frac{\boldsymbol{F}}{m} \tag{4}$$

where GM_p is the gravitational parameter of the planet, $\boldsymbol{r}_p$ is the third-body position vector, and $\boldsymbol{r}_{sp}$ is the spacecraft to third-body vector; all vectors are in the ECLIPJ2000 frame. In addition to the position and velocity, the mass of the spacecraft is also propagated as an additional ODE, given by

$$\dot{m} = -\frac{F}{g_0 I_{sp}} \tag{5}$$

The CR3BP equations of motion are given by

$$\ddot{x} - 2\dot{y} = \frac{\partial U}{\partial x}\ ,\ \ddot{y} + 2\dot{x} = \frac{\partial U}{\partial y}\ ,\ \ddot{z} = \frac{\partial U}{\partial z} \tag{6}$$

where U is the pseudo-potential given by

$$U = \frac{x^2 + y^2}{2} + \frac{1-\mu}{r_1} + \frac{\mu}{r_2} \tag{7}$$

and μ is the mass-parameter of the Sun-planet system, given by

$$\mu = \frac{M_p}{M + M_p} \tag{8}$$

Libration Point Orbits and Manifolds

LPOs are periodic orbits in the CR3BP that revolve around libration points. Given a state along the LPO $\mathbf{x}_0$, its invariant manifolds may be obtained by perturbing states on the LPO along the local stable or unstable eigenvector direction. Starting with $\mathbf{x}_0$ and LPO period P, the state-transition matrix STM, Φ is obtained from the initial value problem

$$\dot{\Phi} = A\Phi \tag{9}$$

$$\Phi(0) = \mathbf{I}_{6,6} \tag{10}$$

where the A matrix is given by

$$A(\mathbf{x}, t) = \left[\begin{array}{c|c} \mathbf{0}_{3,3} & \mathbf{I}_{3,3} \\ \hline U_{\mathbf{xx}} & 2\boldsymbol{\Omega} \end{array}\right]\ ,\ \boldsymbol{\Omega} = \begin{bmatrix} 0 & 1 & 0 \\ -1 & 0 & 0 \\ 0 & 0 & 0 \end{bmatrix} \tag{11}$$

where $U_{\mathbf{xx}}$ is a 3-by-3 matrix consisting of second order partial derivatives of U. Then, the stable and unstable eigenvectors of the problem, Y^s and Y^u, are obtained from solving the eigenvalue problem for the monodromy matrix $\Phi(P)$. Then, the initial condition of the stable and unstable manifold branches are obtained by perturbing the state along the LPO in the eigenvector direction with some magnitude ϵ.

$$\mathbf{x}^s_{ptb}(t_{\text{LPO}}) = \mathbf{x}_0(t_{\text{LPO}}) \pm \epsilon \mathbf{Y}^s(t_{\text{LPO}}) \tag{12}$$

$$\mathbf{x}^u_{ptb}(t_{\text{LPO}}) = \mathbf{x}_0(t_{\text{LPO}}) \pm \epsilon \mathbf{Y}^u(t_{\text{LPO}}) \tag{13}$$

where t_{LPO} denotes the time along the LPO, and $0 \leq t_{\text{LPO}} \leq P$. The stable branches are obtained by backward propagation of the initial state $\mathbf{x}^s_{ptb}(t_{\text{LPO}})$, while the unstable branches are obtained by forward propagation of the initial state $\mathbf{x}^u_{ptb}(t_{\text{LPO}})$. Figure 1 shows an example of stable and unstable manifolds for a Sun-Venus L2 halo orbit.

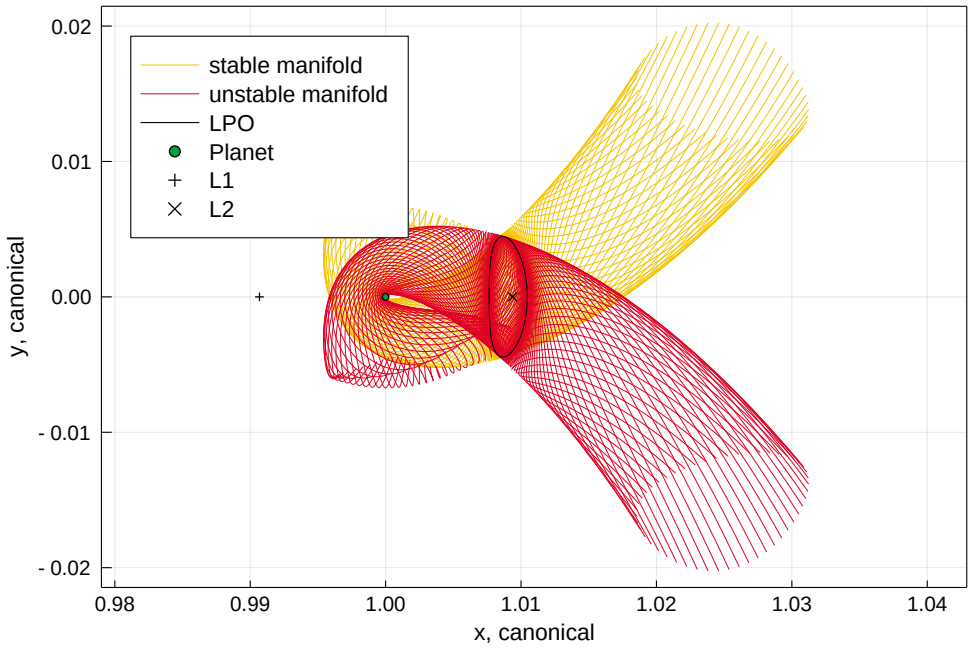

Figure 1. Sun-Venus L2-halo orbit, stable, and unstable manifold

PROPOSED METHOD

The LPO-capture segment is incorporated into the interplanetary trajectory design problem by modifying the transcription of the arrival parameters from a traditional SFT. The problem is solved with a gradient-based solver wrapped by a global search pseudo-algorithm.

Sims-Flanagan Transcription

The conventional SFT considers an interplanetary trajectory in terms of N *legs*, connecting two consecutive planetary bodies visited by the spacecraft. At each planetary visit, a *control-node* is defined based on the ephemeris of the planet at a given epoch and an associated v_∞ vector. In case of a fly-by control-node, two v_∞ vectors are defined for the in-coming and out-going legs, respectively. Over each leg, the control-nodes at both ends are propagated forward and backward in time for half of the flight-time of the leg, and the final states of each propagation are denoted as the forward and backward *patch-points*. The optimizer must drive the residual at the *patch-point* to 0 by tuning the control-nodes along with the thrust controls.

For the propagation, each leg is is discretized into n equal-time *segments*, over which the thrust control is kept constant. The original formulation involves further simplifying the propagation by considering Keplerian arcs with an impulsive ΔV at the center of each segment to approximate the low-thrust maneuver.[7] While this has been implemented in multiple tools such as MALTO[8] and GALLOP,[14] propagation based integration of the two-body equations of motion has also been proposed as a higher-fidelity approach.[15]

Problem Objective and Decision Vector The trajectory optimization problem may be formulated to maximize the final mass

$$\min_{\boldsymbol{x}} \; -m^{N+1} \tag{14}$$

for the decision vector $\boldsymbol{x}$ given by

$$\boldsymbol{x} = [\boldsymbol{g}_{\text{launch}},\, \boldsymbol{g}^1_{\text{fly-by}},\, \ldots,\, \boldsymbol{g}^{N-1}_{\text{fly-by}},\, \boldsymbol{g}_{\text{arrival}},\, \boldsymbol{\nu}^1,\, \ldots,\, \boldsymbol{\nu}^N] \tag{15}$$

where $\boldsymbol{g}$ are parameters at the initial, intermediate, and final nodes along the transfer, and $\boldsymbol{\nu}$ are the discretized controls of the thruster for each leg between $j = 1, \ldots, N$. For any mission, the launch parameter $\boldsymbol{g}_{\text{launch}}$ is given by

$$\boldsymbol{g}_{\text{launch}} = [t, m^1, v^1_\infty, \alpha^1, \delta^1] \tag{16}$$

representing, in order, the launch epoch, mass, v_∞ magnitude, right-ascension, and declination at launch. If the transfer has gravity assist(s) along its way, there will also be one or more fly-by parameters $\boldsymbol{g}_{\text{fly-by}}$, given by

$$\boldsymbol{g}^i_{\text{fly-by}} = [\Delta t^i, m^{i+1}, v^{i+1}_\infty, \alpha^{i+1}_-, \delta^{i+1}_-, \alpha^{i+1}_+, \delta^{i+1}_+]\,, \;\; i \in [1, N-1] \tag{17}$$

where the superscript i represents the i^{th} visited body by the spacecraft after launch. In this case, the epoch from $\boldsymbol{g}_{\text{launch}}$ is replaced by the time-of-flight since the last visited node, given by Δt^i. There are also pairs of right-ascension and declination, $\alpha^i_\pm$ and $\delta^i_\pm$, corresponding to the in-coming and out-going values. If powered fly-by's are also to be considered, there should also be a pair of v^i_∞ values. Finally, the arrival parameters $\boldsymbol{g}_{\text{arrival}}$ are given by

$$\boldsymbol{g}_{\text{arrival}} = [\Delta t^N, m^{N+1}, v^{N+1}_\infty, \alpha^{N+1}, \delta^{N+1}] \tag{18}$$

which consists of the same components as the launch parameters except for the epoch, which is now replaced by the time-of-flight since the last visited node.

The thrust control vector $\boldsymbol{\nu}^j$ represents the sequence of controls the thruster must undertake during the j^{th} leg. It is given by

$$\boldsymbol{\nu}^j = [\tau^j_1,\, \theta^j_1,\, \beta^j_1,\, \ldots,\, \tau^j_k,\, \theta^j_k,\, \beta^j_k,\, \ldots,\, \tau^j_n,\, \theta^j_n,\, \beta^j_n]\,, \;\; j \in [1, N]\;, k \in [1, n] \tag{19}$$

where τ is the up-to-unit thrust throttle, θ is the in-plane, and β is the out-of-plane control angle, which are defined in the local-vertical local-horizontal (LVLH) frame.

Bounds on the Decision Vector Each component of the decision vector are bounded by lower and upper bounds. The launch epoch t is bounded by the desirable launch window for a mission. The masses m are bounded between 0 and 1, when non-dimensionalizing the problem using the wet-mass. The time of flights between two consecutive bodies are bounded by considering the orbital periods of the planets at the forward and backward control-nodes, as suggested by Englander and Englander;[16] considering the orbital periods P_{fwd} and P_{bck} and semi-major axes a_{fwd} and a_{bck} of the forward and backward planets, lower-bound is given by

$$\Delta t_{\text{lb}} = \begin{cases} \dfrac{P_{\text{fwd}}}{2}\,, \text{leg between same planet} \\ 0.1 \min(P_{\text{fwd}}, P_{\text{bck}})\,, \text{otherwise} \end{cases} \tag{20}$$

and the upper-bound is given by

$$\Delta t_{\text{ub}} = \begin{cases} 5P_{\text{fwd}}\,, \text{leg between same planet} \\ 2\max(P_{\text{fwd}}, P_{\text{bck}})\,, \max(a_{\text{fwd}}, a_{\text{bck}}) < 2\text{AU} \\ \max(P_{\text{fwd}}, P_{\text{bck}})\,, \max(a_{\text{fwd}}, a_{\text{bck}}) \geq 2\text{AU} \end{cases} \tag{21}$$

The throttle τ is bounded by 0 and 1, while the angles θ and β are bounded between $-\pi$ and π. The v_∞ magnitude is bounded between 0 and a multiple of the parabolic excess velocity in the heliocentric frame at a distance $\max(a_{\text{fwd}}, a_{\text{bck}})$ from the Sun. The two associated angles α and δ are again bounded between $-\pi$ and π.

Problem Constraints The constraints of this problem consists of the patch-point constraint(s), c_{mp}, time of flight constraint, c_{tof}, and fly-by altitude constraint(s), $c_{\text{fly-by}}$. The patch-point constraint is an equality constraint which consists of the residuals from the forward and backward propagation of the control-nodes; this is computed for each leg of the transfer, and is given by

$$\boldsymbol{c}_{mp}^{j} = s_{\text{bck}} - s_{\text{fwd}} = 0\,, \quad j \in [1, N] \tag{22}$$

where s_{fwd} and s_{bck} are the forward and backward propagation of the position, velocity, and mass. The time-of-flight constraint is an inequality constraint to ensure the spacecraft arrives to its intended destination within a predefined duration, tof_{max}. It is given by the summation of the time of flights for each segment

$$c_{\text{tof}} = tof - tof_{max} = \sum_{j=1}^{N} \Delta t_j - tof_{max} \leq 0 \tag{23}$$

The fly-by altitude constraint is also an inequality constraint which ensures a minimum safety altitude, h_{safe} , when a spacecraft conducts a gravity-assist. For each gravity-assist, this constraint is defined as

$$c_{\text{fly-by}} = \left(r_{\text{planet}} + h_{\text{safe}}\right) - \frac{\mu_{\text{planet}}}{v_\infty^2}\left[1/\sin\left(\frac{\delta_{\text{turn-angle}}}{2}\right) - 1\right] \leq 0 \tag{24}$$

where $\delta_{\text{turn-angle}}$ is the turn-angle around the planet

$$\delta_{\text{turn-angle}} = \arccos\left(\frac{\boldsymbol{v}_\infty^- \cdot \boldsymbol{v}_\infty^+}{v_\infty^- v_\infty^+}\right) = \arccos\left(\frac{\boldsymbol{v}_\infty^- \cdot \boldsymbol{v}_\infty^+}{v_\infty^2}\right) \tag{25}$$

The denominator may be simplified if the fly-by is not powered, since the incoming and outgoing v_∞ vectors must have equal magnitudes. This is computed at each fly-by control-node, $\boldsymbol{g}_{\text{fly-by}}^{i}$.

Modifications to Arrival Parameters for Targeting Libration Point Orbits

To incorporate ballistic arrivals into LPOs, the arrival parameters (18) must be replaced by one that approximates the spacecraft's state in a three-body regime. To this end, the stable manifold of the LPO is utilized; instead of starting the final backward segment of the trajectory from the ephemeris of the planet, the control-node is set on a state-vector lying on a PS that is a cross-section of the manifold. This ensures the spacecraft to insert into the LPO on a ballistic path along the manifold. Since the control-node no longer represents an arrival to a planetary body, such arrival control node does not have an associated v_∞ value.

Two approaches to formulate such PS-based arrival parameters are considered; the first involves pre-defining a specific PS in the CR3BP frame, while the second involves letting the optimizer choose a PS based on lower and upper bounds on the time spent on the manifold between the PS and the LPO. The former is denoted as the fixed-PS arrival, while the latter is denoted as the free-PS arrival.

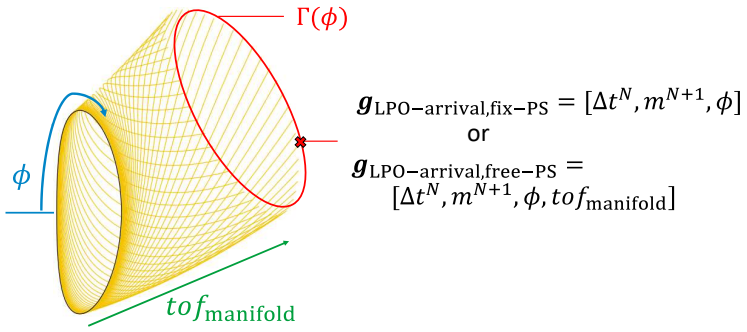

Figure 2. Representation of arrival condition at the libration point orbit via stable manifold

Targeting Libration Point Orbit at Fixed Poincaré Section In the fixed-PS arrival case, the PS may be parameterized by a single parameter ϕ, which may be understood as the location around the LPO to which a manifold branch is connected. Then, the cross-section of the manifold may be parameterized as a curve Γ, which takes in ϕ and returns the corresponding position and velocity on the PS. These are shown in Figure 2. Then, the arrival parameters from expression (18) is replaced by

$$\boldsymbol{g}_{\text{LPO-arrival, fixed-PS}} = \left[\Delta t^N, m^{N+1}, \phi\right] \tag{26}$$

where the terms Δt^N and m^{N+1} remain the same as for the $v_\infty > 0$ case from the nominal case. Given these arrival parameters, the control-node is computed by the following algorithm:

Algorithm 1: Evaluation of control-node for fixed-PS arrival

Result: Control-node in ECLIPJ2000 frame
given Γ, arrival parameters $\boldsymbol{g}_{\text{LPO-arrival, fixed-PS}} = \left[\Delta t^N, m^{N+1}, \phi\right]$
obtain control-node position and velocity in CR3BP frame via $\boldsymbol{S}^{\text{CR3BP}} = \Gamma(\Phi)$
transform control-node from CR3BP to ECLIPJ2000 via $\boldsymbol{S}^{\text{ECLIPJ2000}} = \boldsymbol{T}_{\text{EC}}(t^N)\boldsymbol{S}^{\text{CR3BP}}$

Targeting Libration Point Orbit at Free Poincaré Section In the free-PS arrival case, an additional parameter is required to first construct the PS that cuts through a manifold. In this case, the arrival parameters are given by

$$\boldsymbol{g}_{\text{LPO-arrival, free-PS}} = \left[\Delta t^N, m^{N+1}, \phi, tof_{\text{manifold}}\right] \tag{27}$$

where tof_{manifold} is the time spent in the capture segment of the manifold. Again, the parameters are shown in Figure 2. It is also noted that the time of flight constraint must be modified to also include

$$c_{\text{tof}} = tof + tof_{\text{manifold}} - tof_{max} = \sum_{j=1}^{N} \Delta t_j - tof_{max} \leq 0 \tag{28}$$

Algorithm 2: Evaluation of control-node for free-PS arrival

Result: Control-node in ECLIPJ2000 frame
given arrival parameters $\boldsymbol{g}_{\text{LPO-arrival, free-PS}} = \left[\Delta t^N, m^{N+1}, \phi, tof_{\text{manifold}},\right]$
construct PS by propagating stable manifold by tof_{manifold}
construct curve Γ along the manifold cross-section at the PS
obtain control-node position and velocity in CR3BP frame via $\boldsymbol{S}^{\text{CR3BP}} = \Gamma(\Phi)$
transform control-node from CR3BP to ECLIPJ2000 via $\boldsymbol{S}^{\text{ECLIPJ2000}} = \boldsymbol{T}_{\text{EC}}(t^N)\boldsymbol{S}^{\text{CR3BP}}$

Modification to Propagation of Segments

While typical SFT formulation propagates segments using Kepler's equation, the approach taken in this work integrates the two-body equations of motion.[15] Then, instead of applying impulsive burns at each segment, a continuous thrust force is applied in at a constant throttle and angle in the LVLH frame. To account for ballistic arrival, the third-body perturbation due to the final encountered body of the mission is incorporated into the equations of motion for the final leg; thus, the equation of motion is given by

$$\ddot{\boldsymbol{r}}^j = \begin{cases} \text{equation (4)}\,, j = N \\ \text{equation (3)}\,, \text{otherwise} \end{cases} \tag{29}$$

Algorithmic Summary

The modified version of the SFT is implemented in Julia. An algorithmic summary to evaluate the constraints of the problem is as follows:

Algorithm 3: Evaluation of Trajectory in Modified Sims-Flanagan Transcription

Result: Evaluate constraints $\boldsymbol{c}_{mp}^j$, c_{tof}, $c_{\text{fly-by}}$
evaluate c_{tof} via equation (23)
for $j = 1$ *to* N **do**
  compute segment-wise time-of-flight $\Delta t_{\text{seg}} = \Delta t_j / n$
  Set forward control-node from ephemeris of planet $\boldsymbol{S}_{\text{fwd}}$
  if $j \neq N$ **then**
    set backward control-node from ephemeris of planet $\boldsymbol{S}_{\text{bck}}$
    set equations of motion to (3);
  else
    set backward control-node via Algorithm 1 or 2
    set equations of motion to (4);
  end
  initialize forward state with control-node $\boldsymbol{s}_{\text{fwd}}^0 \leftarrow \boldsymbol{S}_{\text{fwd}}$
  initialize backward state with control-node $\boldsymbol{s}_{\text{bck}}^0 \leftarrow \boldsymbol{S}_{\text{bck}}$
  for $k = 1$ *to* $n/2$ **do**
    set forward segment thrust controls $\boldsymbol{\nu}_{\text{fwd}}^j = [\tau_k^j, \theta_k^j, \beta_k^j]$
    set backward segment thrust controls $\boldsymbol{\nu}_{\text{bck}}^j = [\tau_{n/2-k+1}^j, \theta_{n/2-k+1}^j, \beta_{n/2-k+1}^j]$
    propagate forward $\boldsymbol{s}_{\text{fwd}}^0$ by Δt_{seg} to get $\boldsymbol{s}_{\text{fwd}}^1$
    propagate backward $\boldsymbol{s}_{\text{bck}}^0$ by $-\Delta t_{\text{seg}}$ to get $\boldsymbol{s}_{\text{bck}}^1$
    set $\boldsymbol{s}_{\text{fwd}}^0 \leftarrow \boldsymbol{s}_{\text{fwd}}^1$
    set $\boldsymbol{s}_{\text{bck}}^0 \leftarrow \boldsymbol{s}_{\text{bck}}^1$
  end
  evaluate patch-point constraint $\boldsymbol{c}_{mp}^j = \boldsymbol{s}_{\text{bck}}^1 - \boldsymbol{s}_{\text{fwd}}^1$
end

Optimization Method

The evaluation of the objective of a SFT problem is trivial, since the final mass m^N is part of the decision vector. In contrast, the evaluation of the constraints are more involved, and as such the difficulty of the problem arises in obtaining feasible solutions. Furthermore, the design

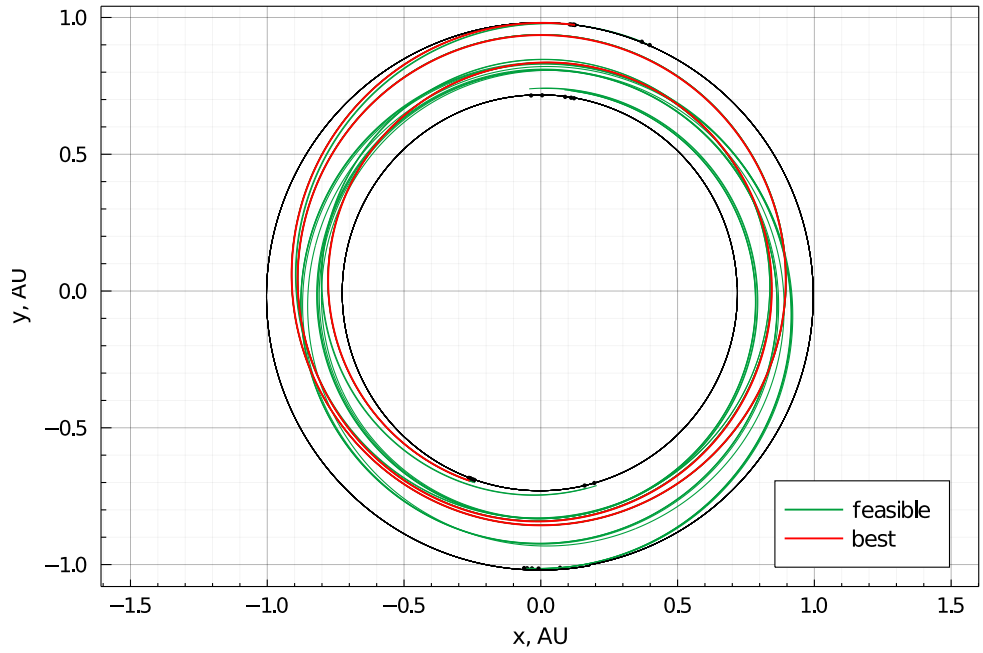

Figure 3. Heliocentric portion of Earth-Venus transfer with fixed Poincaré section

space typically consists of multiple local optima. To tackle these challenges, a common approach consists of wrapping a local gradient-based search method with a monotonic basin hopping pseudo-algorithm (MBH) for global exploration of the trade-space. While gradient-based methods such as SNOPT[17] and IPOPT[18] successfully drive the decision vector to a feasible solution. MBH has been initially introduced by Wales and Doye[19] for optimizing a problem with a funnel structure, and has since been found to be particularly effective by multiple authors for interplanetary trajectory design problems.[16,20–22]

OPTIMIZATION RESULTS

As an example, a low-thrust transfer from Earth to Venus, inserting into a Venus-L2 halo orbit of out-of-plane amplitude 150,000 km is considered. The launch epoch is chosen between January 1^{st}, 2022, and December, 31^{st}, 2024, and the upper bound on the time of flight is set to 2 years. The thruster is set to have an Isp of $3500\,\mathrm{seconds}$ and constant maximum thrust of $0.4\,\mathrm{Newtons}$, and a wet mass of $4100\,\mathrm{kg}$ is considered. The SFT problem is constructed using $n = 20$ segments in each leg. As a point of comparison, a regular SFT Earth-Venus transfer problem arriving to Venus with $v_\infty = 0$, corresponding to a parabolic approach, is also solved. For all cases, planetary ephemerides are taken from JPL's de440 bsp file.

For the fixed-PS case, the PS is defined based on backward-propagation of the branches by 100 days from the LPO. Transfers found for the fixed-PS arrival case are shown in Figures 3 and 4, respectively for the heliocentric and ballistic capture portions of the transfer. All *feasible* solutions found by local optimizer runs are shown in green, and the best solution among these is shown in blue. For the free-PS case, bounds on the PS location is bounded such that tof_{manifold} is between 80 and 100 days from the LPO. Transfers for the free-PS case are shown in Figures 5 and 6, again for the heliocentric and ballistic capture portions, respectively.

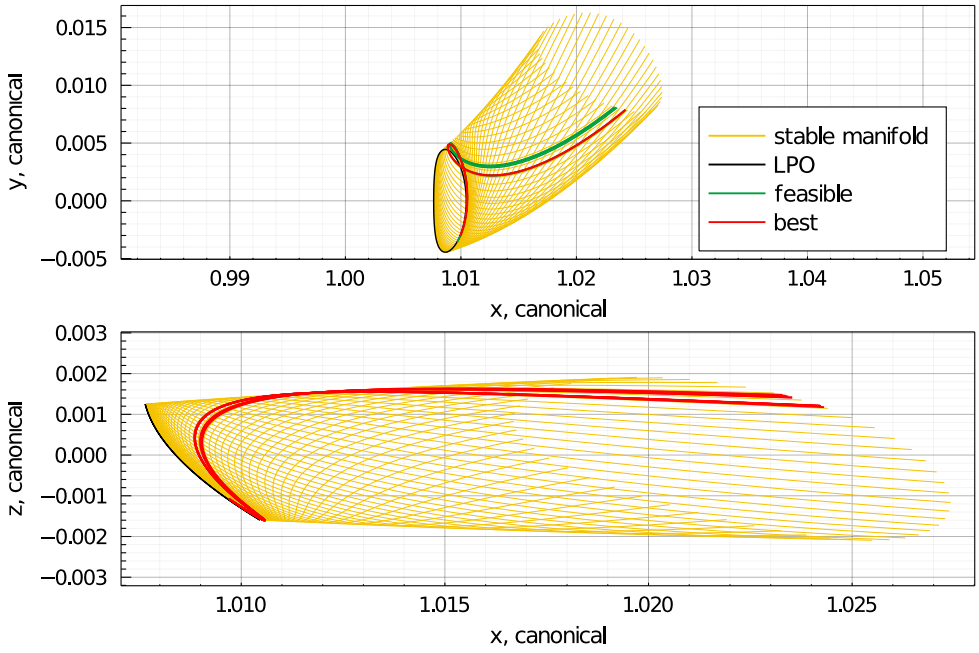

Figure 4. Ballistic capture portion of Earth-Venus transfer with fixed Poincaré section

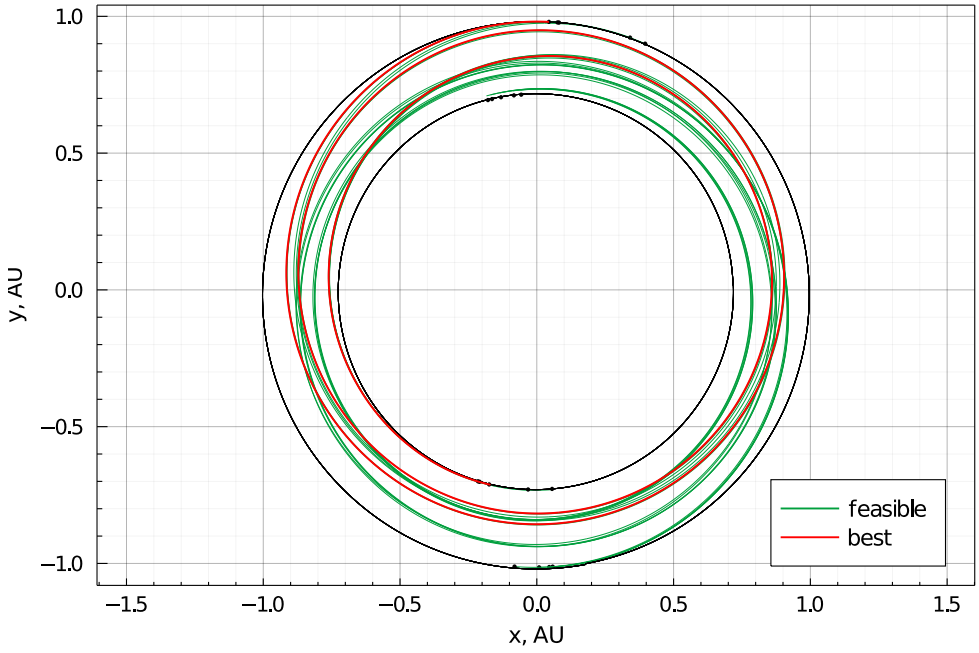

Figure 5. Heliocentric portion of Earth-Venus transfer with free Poincaré section

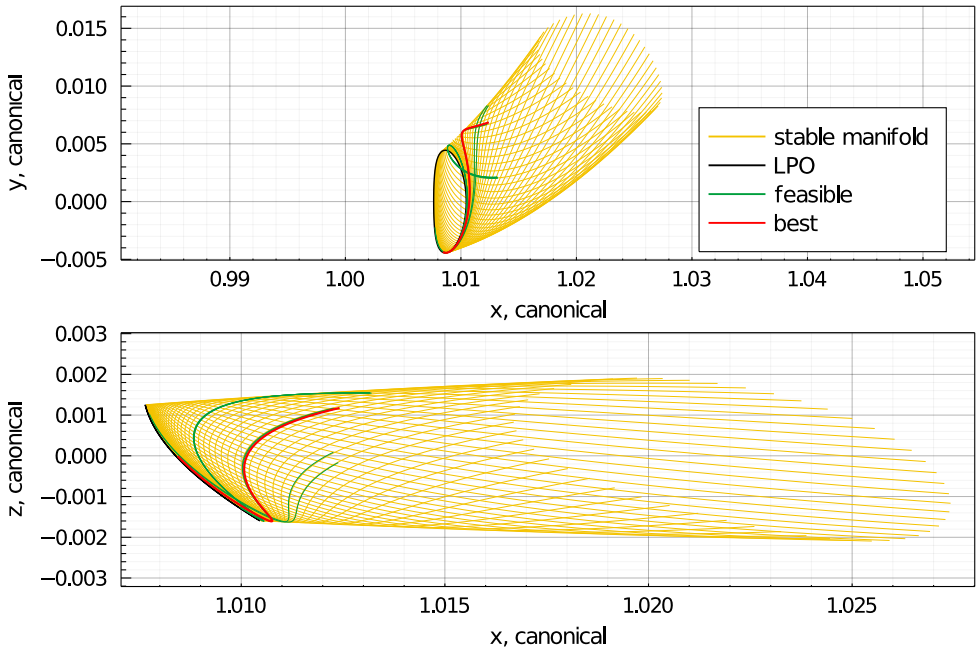

Figure 6. Ballistic capture portion of Earth-Venus transfer with free Poincaré section

When given the flexibility, it has been observed that the optimizer favors insertion into the manifold at the latest possible time, or equivalently spending the shortest allowable amount of time on the manifold, at around 84 days. Figure 7 compares the obtained solutions for the fixed-PS and free-PS cases against a traditional SFT formulation with a parabolic arrival. The converged delivered mass when solving the problem for a parabolic arrival is unanimously lower than the fixed-PS and free-PS cases; for preliminary design of missions leveraging LPOs, it is therefore preferable to utilize the proposed method, which leads to a better initial estimation of the required propellant mass.

While not covered within the scope of this paper, the ballistic capture segment may also be defined in the elliptic restricted three body problem (ER3BP) for cases inserting into LPOs around highly elliptical Sun-planet systems such as Mercury. Similar arrival conditions may also be envisioned for generic WSBC captures, such as low-thrust spirals around a body, by parameterizing the feasible ballistic entries in a similar approach, allowing the optimizer to tune these parameters.

CONCLUSION

The proposed method in this work builds on the SFT, which has previously been found to be a reliable approach for designing low-thrust interplanetary transfers, and extends it with the incorporation of ballistic captures to LPOs. This enables the design of transfers that may be fully executed using EP, as impulsive maneuvers are not necessary. This is made possible via the modification of the parameters that characterize the arrival at the destination, namely from a v_∞ vector to a set of variables that parameterize an insertion point into a manifold. To avoid having a discontinuities in the dynamics, Kepler's equation based propagation is replaced with an integration of two-body ODE with a third-body perturbation. As both crewed and robotic deep-space exploration missions are expected to increase in decades to come, end-to-end EP-compatible transfer designs will become

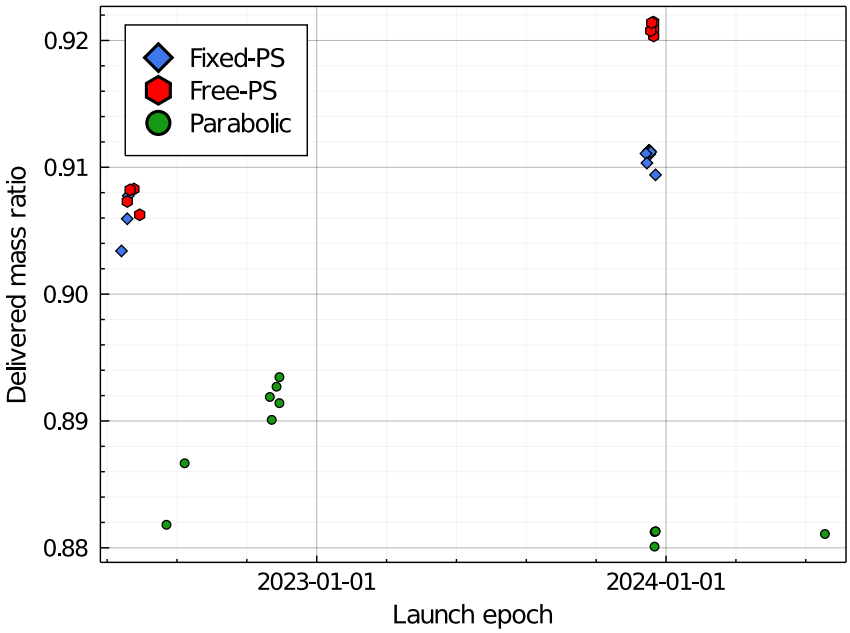

Figure 7. Scatter of solutions found

a key enabling strategy in sending large payload mass. The approach presented in this work lays out the necessary strategy for designing such interplanetary transfers that arrives to a LPO. Certain mission objectives may be well-suited for a spacecraft located in a LPO, while it may also be used as a staging orbit before inserting into orbits closer to the primary. Finally, the proposed approach may be extended for designs of transfers culminating in more generic WSBC as well.

REFERENCES

[1] R. Jehn, S. Campagnola, D. Garcia, and S. Kemble, "Low-thrust approach and gravitational capture at Mercury," *European Space Agency, (Special Publication) ESA SP*, No. 548, 2004, pp. 487–492.

[2] D. G. Yarnoz, R. Jehn, and P. De Pascale, "Trajectory design for the Bepi-Colombo mission to mercury," *57th International Astronautical Congress*, Vol. 7, 2006, pp. 4712–4719, 10.2514/6.iac-06-c1.8.07.

[3] H. Pernicka, D. Henry, and M. Chan, "Use of halo orbits to provide a communication link between earth and Mars," *AIAA/AAS Astrodynamics Conference*, 1992, pp. 445–455, https://doi.org/10.2514/6.1992-4585.

[4] J. D. Strizzi, J. M. Kutrieb, P. E. Damphousse, and J. P. Carrico, "Sun-Mars libration points and Mars mission simulations," *AAS/AIAA Astrodynamics Specialist Conference*, 2001, pp. 807–822.

[5] Y. Tanaka, Y. Kawakatsu, and H. Yoshimura, "Design of Escaping Trajectory from Mars by Using a Halo Orbit as Hub and a Method of Delta V Reduction," *The 28th Workshop on JAXA Astrodynamics and Flight Mechanics*, 2018, pp. 3–8.

[6] M. Shirobokov, S. Trofimov, and M. Ovchinnikov, "On the design of a space telescope orbit around the Sun–Venus L2 point," *Advances in Space Research*, Vol. 65, No. 6, 2020, pp. 1591–1606, 10.1016/j.asr.2019.12.022.

[7] J. A. Sims and N. Flanagan, "Preliminary design of low-thrust interplanetary missions," *AAS Astrodynamics Specialists Conference*, 1999.

[8] J. Sims, P. A. Finlayson, E. Rinderle, M. A. Vavrina, and T. D. Kowalkowski, "Implementation of a Low-Thrust Trajectory Optimization Algorithm for Preliminary Design," 2006.

[9] R. T. Eapen and R. K. Sharma, "Mars interplanetary trajectory design via Lagrangian points," *Astrophysics and Space Science*, Vol. 353, No. 1, 2014, pp. 65–71, 10.1007/s10509-014-2012-x.

[10] E. Belbruno and F. Topputo, "Earth – Mars transfers with ballistic capture," 2015, pp. 329–346, 10.1007/s10569-015-9605-8.

[11] F. Topputo, M. Vasile, and F. Bernelli-Zazzera, "Low energy interplanetary transfers exploiting invariant manifolds of the restricted three-body problem," *Journal of the Astronautical Sciences*, Vol. 53, No. 4, 2005, pp. 353–372, 10.1007/bf03546358.

[12] Y. Shimane, "Periapsis Targeting with Weak Stability Boundary Transfers for Orbiting Around Planetary Moons," *AAS Space Flight Mechanics Meeting*, 2021, pp. 1–12.

[13] N. Hyeraci and F. Topputo, "Method to design ballistic capture in the elliptic restricted three-body problem," *Journal of Guidance, Control, and Dynamics*, Vol. 33, No. 6, 2010, pp. 1814–1823, 10.2514/1.49263.

[14] T. McConaghy, T. J. Debban, A. Petropoulos, and J. Longuski, "Design and Optimization of Low-Thrust Trajectories with Gravity Assists," *Journal of Spacecraft and Rockets*, Vol. 40, 2003, pp. 380–387.

[15] C. H. Yam, D. Izzo, and F. Biscani, "Towards a High Fidelity Direct Transcription Method for Optimisation of Low-Thrust Trajectories," *4th International Conference on Astrodynamics Tools and Techniques.*, 2010, pp. 1–7.

[16] J. A. Englander and A. C. Englander, "Tuning Monotonic Basin Hopping: Improving the Efficiency of Stochastic Search as Applied to Low-Thrust Trajectory Optimization," *International Symposium on Space Flight Dynamics 2014*, 2014, pp. 1–33.

[17] P. E. Gill, W. Murray, and M. A. Saunders, "SNOPT: An SQP algorithm for large-scale constrained optimization," *SIAM Review*, Vol. 47, No. 1, 2005, pp. 99–131, 10.1137/S0036144504446096.

[18] A. Wächter and L. T. Biegler, "On the implementation of an interior-point filter line-search algorithm for large-scale nonlinear programming," *Mathematical Programming*, Vol. 106, No. 1, 2006, pp. 25–57, 10.1007/s10107-004-0559-y.

[19] D. J. Wales and J. Doye, "Global Optimization by Basin-Hopping and the Lowest Energy Structures of Lennard-Jones Clusters Containing up to 110 Atoms," *The Journal of Physical Chemistry A.*, Vol. 101, No. 28, 1997, pp. 5111–5116.

[20] C. H. Yam, D. Izzo, and D. D. Lorenzo, "Low-thrust trajectory design as a constrained global optimization problem," *Proceedings of the Institution of Mechanical Engineers, Part G: Journal of Aerospace Engineering*, Vol. 225, No. 11, 2011, pp. 1243–1251, 10.1177/0954410011401686.

[21] D. Izzo, "PyGMO and PyKEP: Open Source Tools for Massively Parallel Optimization in Astrodynamics (the case of interplanetary trajectory optimization)," 01 2012.

[22] S. L. McCarty and M. L. McGuire, "Parallel monotonic basin hopping for low thrust trajectory optimization," *Space Flight Mechanics Meeting, 2018*, No. 210009, 2018, 10.2514/6.2018-1452.